First-Principles Study of Adsorption of Methane on Defective Silicene

T. Adhikari, N. Pantha, and N. Adhikari

Journal of Nepal Physical Society
Volume 8, No 2, 2022
(Special Issue: ANPA Conference 2022)
ISSN: 2392-473X (Print), 2738-9537 (Online)

JNPS, **8** (2), 7-13 (2022)
DOI: http://doi.org/10.3126/jnphyssoc.v8i2.50139

Published by: Nepal Physical Society
P.O. Box: 2934
Tri-Chandra Campus
Kathmandu, Nepal
Email: nps.editor@gmail.com

ANPA Conference 2022
ISSN : 2392-473X(Print), 2738-9537 (Online)

DOI:http://doi.org/10.3126/jnphyssoc.v8i2.50139

First-Principles Study of Adsorption of Methane on Defective Silicene

T. Adhikari,[a] N. Pantha,[b] and N. Adhikari[c]

Central Department of Physics, Tribhuvan University, Kathmandu Nepal

[a] *tbndhkr@gmail.com*
[b] *mrnurapati@gmail.com*
[c] *narayan.adhikari@cdp.tu.edu.np*

Abstract. Considering the significance of natural gas, such as methane, and the difficulties in storing it, research is increasingly focusing on developing materials for solid-state methane storage. Two-dimensional materials have a large number of possible adsorption sites for gas molecules due to their high surface-to-volume ratio. However, the two-dimensional structure is chemically inactive and attracts nonpolar gases rather weakly. We investigated the methane gas adsorption capabilities of silicene by activating it with different defects. According to our density functional theory calculations, the mono-vacancy (MV) defect is advantageous in increasing the binding strength of energy-carrying gases such as methane. In MV defective silicene, methane adsorption energy is detected in the order of the internationally specified energy regime.

Received: 24 August 2022; **Accepted**: 06 November 2022; **Published**: 31 December 2022

Keywords: DFT; silicene; Mono-vacancy; Stone-Wales.

INTRODUCTION

Existence of two dimensional (2D) crystal was thought impossible for many years. It was considered that they would ultimately changed back to three dimensional (3D) form [1]. Presence of thermal fluctuation cause atomic displacements of same magnitude as the atomic distance make 2D form unstable. But now scenarios is completely different, almost 700 2D materials have been predicted to be stable, very few of them being synthesized till date [2]. The discovery of graphene provides the breakthrough for the advancement in the field of research and stimulates a strong effort to search theoretically and experimentally for similar 2D materials [3]. As a result, silicene the graphene equivalent of silicon was mentioned in the theoretical study of Takeda and Shiraishi in 1994 [4] and then re-investigated by Guzman-Verri *et al.* [5] in 2007, who named it silicene has followed the trend, opening new perspectives for applications, especially because of its compatibility with Si-based electronics. In 2009 low buckled geometries were confirmed to be dynamically stable through ab-initio calculations [6]. Despite such low-buckled structure silicene shared must of the outstanding electronic properties of graphene. Much stronger spin-orbit coupling, better tunability of bandgap, easier valley polarization and more suitability of valleytronics are prominent advantages of silicene over graphene [7].

The presence of zero bandgap characters of silicene hinders its applications in nano-electronic and opto-electronic devices. Thus it is desirable to open a finite bandgap in silicene. And hydrogenation can convert sp^2 hybridized silicene to sp^3 and provide a simple way to fulfill the goal of gap opening [8]. This shows that small modifications in structure influence the drastic change in the properties. Stone-Wales (SW) defect is the common topological defect that is obtained on 90^0 rotation of Si-Si bond along with the formation of two heptagonal and two pentagonal rings. For the infinite silicene sheet formation energy of SW rotation from DFT calculation is 209 eV [9]. The existence of SW defect induces tiny bandgap 33meV by breaking hexagonal symmetry for 5×5 supercell [9]. It means the presence of the SW defect would open a small bandgap without losing the high carrier velocity that can be of great importance in nano-electronics. Vacancies defect arise from missing one or few lattice atoms in 2D honeycomb crystal. In study of infinite silicene sheet modeled by (5×5) supercell, mono-vacancy (MV) defect transform semimetallic silicene to metallic,

a types of di-vacancy (DV-1) introduce moderate bandgap of 161 meV, another di-vacancy (DV-2) destroy the Dirac cone with keeping semi-metallic character [9]. In this way, vacancy defects modify the electronic properties of silicene effectively.

Among various 2D materials, silicene is shown to be stable when alternating atoms of hexagons are buckled. Theoretical and experimental studies of silicene suggest that silicene grown on Ag(111) substrate is stable but local defects can always exist at finite temperature. And on further studies it was found that chemical activity is increased on the adsorption of foreign atoms at the defected sites, even specific gas can dissociate into its constituents [9]. silicene's high reactivity not only results in robust adherence to the substrate, but it also results in quick breakdown of the silicene device when exposed to ambient air. As a result, a viable silicene device must seek protection from ambient air. More research on silicene is required to investigate its possible uses in gas detection. In addition, study of N. Pantha *et al.* [10] on methane adsorption on graphene, defects on (hexagonal Boron Nitride) h-BN [11], and changing of structural and electronic properties of phosphorene with defects (vacancies) [12] compelled us to do this research. As a result, we are driven to chose defective silicene as the topic of study, and we are enthusiastic to expand our understanding of small gas molecule adsorption on defective silicene. Here we are aiming to examine the adsorption of CH_4 gas molecules on defective silicene.

COMPUTATIONAL METHOD

We have performed the first principles calculations to investigate the structural stability, the electronic and magnetic properties of pristine silicene as well as Stone-Wales and mono-vacancy defective silicene within the framework of density functional theory [13, 14, 15, 16] with van der Waals (vdW) interactions in XDM [17] technique with DFT approach using Quantum ESPRESSO code [18, 19, 20]. To incorporate the electronic exchange and correlation effect in our system, the generalized gradient approximation (GGA) developed by three scientists Perdew, Burke and Ernzerhof (PBE) [21] was used. We used the Kresse-Joubert (KJ) projector augmented wave (PAW) pseudopotential from the Quantum ESPRESSO official website [22] to replace the complicated effects of the motion of an atom's core (*i.e.*, non-valence) electrons with an effective potential, so that only the chemically active valence electrons were explicitly included in our entire calculation. For plane wave expansion kinetic energy cutoff of 45 Ry is used and to prevent the interaction between two consecutive layers space of 20 Å is maintained. Along with that, we use K-points of $4 \times 4 \times 1$, for 5×5 silicene supercell for the measurement of our discrete grid to represent the continuous integral over the brillouin zone. During the calculation, the structure is allowed to relax under Broyden-Fletcher-Goldfarb-Shanno (BFGS) [23] scheme until the total energy change is less than 10^{-4} Ry between two consecutive self consistent field (scf) steps and each component of force acting is less than 10^{-3} Ry/Bohrs to get geometrically optimized structure. Following the relax calculations, we performed a self consistent total energy calculation in which the brillouin zone of silicene is sampled in K-space using the Monkhorst-Pack [24] method with an appropriate number of mesh of K-points established by the convergence test. Also, we have used 'Fermi-Dirac (F-D)' [25] method of smearing with a small smearing width of 0.001 Ry. In addition, for self consistency, we used the 'David' diagonalization technique with the 'plain' mixing mode and a mixing factor of 0.5. We incorporate Bader method of charge transfer analysis to investigate the how charge density is changed due to adsorption of CH_4 gas molecules on all silicene systems [26].

The formula for calculating defect formation energy(E_F) [9] is,

$$\mathbf{E}_F = \mathbf{E}_T - N \times \mathbf{E}_{Si} \tag{1}$$

where E_T is the total energy of defective silicene, N is the number of silicon atoms in the defective silicene supercell, and E_{Si} is the energy per silicon atom in a pristine silicene sheet. Adsorption energy (E_{ad}) is calculated by using following expression;

$$E_{ad} = E_{gas} + E_{system} - E_{gas+system} \tag{2}$$

where, E_{gas} is energy of CH_4 molecule, E_{system} gives the energy of system before gas adsorption and $E_{gas+system}$ gives the energy of system after gas adsorption. Figure 1 (a) shows the unit cell structure of silicene which containing two atoms with the bond length 2.28 Å and Fig. 1(b) shows 5×5 super-cell formed by the propagation of unit cell along the x- and y- directions.

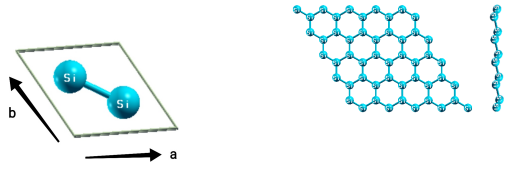

(a) (b)

FIGURE 1: (a) Top view of optimized primitive cell and (b) Top and side view of 5×5 silicene monolayer

RESULTS AND DISCUSSION

We elaborate the formation energy, band structure, density of state (DOS), and partial density of state (PDOS) of pristine and defective i.e, stone-wales, mono-vacancy silicene with and without adsorption of methane gas molecule in this section.

Geometrical structure and formation energy

silicene consists of hexagonal honeycomb structure with unit cell having two atoms placed at each lattice points. Firstly, the unit cell and super-cell are allowed to relax for structural optimization using BFGS quasi-newton algorithm and structural parameters observed in the primitive cell are as shown in Table I. The table also include results from three of the previous studies on silicene i.e, work of Cahangirov *et al*. [6] which is the DFT-LDA approach, Houssa *et al*. [7] DFT-GGA approach and the work of Feng *et al*. [27] an experimental study.

TABLE I: Optimized strucutral parameters of the relaxed primitive silicene. a=b, d and Δ refer to lattice parameter, Si-Si bond length and buckling height of sub-lattices respectively.

Parameters	Obtained values	DFT-LDA [6]	DFT-GGA [7]	Experimental values [27]
(a=b) (Å)	3.87	3.83	3.87	-
(d) (Å)	2.28	2.25	2.28	2.34-2.39
(Δ) (Å)	0.45	0.44	0.44	0.77

After confirming that our work was consistent with earlier work, we prepared the input file for the 5×5 supercell of silicene and then allowed the system to relax. 50 atoms make to the 5×5 supercell of silicene monolayer. It is a unit cell with a 50-atom basis and a cell size five times that of the primitive cell. The outlook for 5×5 supercell is shown in Fig. 1b. After obtaining the appropriate structure and geometry of pure silicene, we remove one of the Si atoms in the centre of the pristine silicene to form a mono-vacancy (MV) defective silicene monolayer, and we rotate one Si-Si bond on pristine silicene by 90^0 to form a Stone-Wales (SW) defective silicene monolayer. As a result of introduction of defect various distortions are observed in Si-Si bond lengths, bond angles etc. The distorted structure due to introduction of defect are presented in Figs. 2a and 2b.

It is seen that distance between Si-Si atoms nearby defected sites is increases upto 2.30 Å in case of vacancy defect. The nearest neighbor bond lengths and bond angles around the site of defect have been constrained by

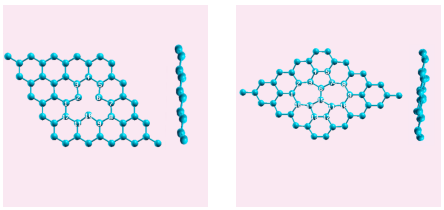

(a) (b)

FIGURE 2: Top view and side view of (a) MV and (b) SW defective silicene

TABLE II: Formation energy, bond-length, bond angles and buckling height of pristine silicene, MV defective silicene and SW defective silicene system respectively.

System	Formation Energy (eV)	bond-length(Å)	bond-angles (^{o})	buckling height (Å)
Pristine		2.28	116.14	0.45
MV	3.44	2.30 - 3.43	105.06 -115.98	0.46
SW	2.05	2.24 - 2.35	116.23 - 135.34	0.38-0.79

some amount as evident in Tables I and II. Similarly, presence of SW defect cause variation in buckling height from 0.38 Å to 0.79 Å which is significant change in comparison to 0.45 Å of pristine silicene sheet. Distortion in bond lengths and angles are also represented in Table II. Along with this, we have found the structural modification in overall sheet, the amount of distortion reducing continuously as we go farther form the doped atom. The formation energy of MV defective silicene is 3.44 eV, which is approximately similar to the prior study's 3.77 eV [9] and that for SW defective system is 2.05 eV almost equivalent to 2.09 eV found in literature [9]. All of the energies in the research are negative, suggesting that the systems are thermodynamically stable. The formation energy of the defective system, on the other hand, is shown to be positive. This suggests that the defective system should be supplied with external energy of that value, demonstrating its unstable nature.

Band structures of silicene system

Using the DFT computation of electronic band structures, we discovered silicene to be a semimetal (zero band gap semiconductor). The valence band maximum (VBM) and conduction band minimum (CBM) touch each other at the K-point of the first brillouin zone (BZ). The π and $\pi*$ bands of silicene are crossed linearly at the Fermi level, resulting in the emergence of massless Dirac fermions, calculated band structures of 5×5 monolayer of pristine silicene is as shown in Fig. 3(a).

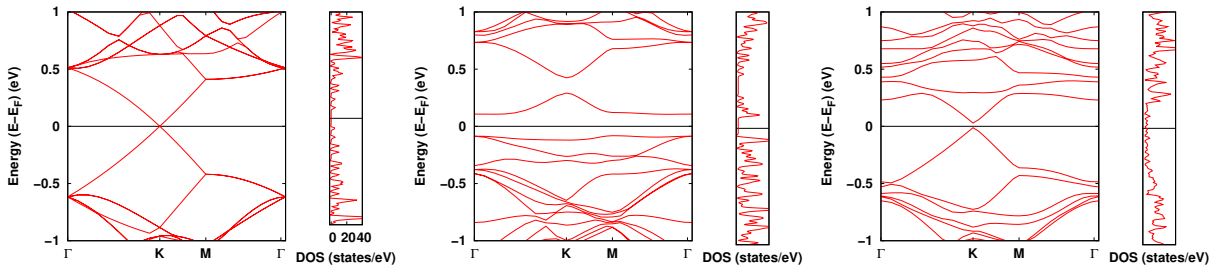

(a) (b) (c)

FIGURE 3: Band structure (with Fermi level set to zero) (a) Pristine silicene, (b) MV defective silicene and (c) SW defective silicene

We discovered considerable changes in band structure as a result of the presence of defects. Figure 3b shows that the bands around the Fermi level are notably different from those in the pristine system. It can also be seen that when mono-vacancy is introduced into a silicene sheet, the system may exhibit metallic behavior, with the Fermi level shifting somewhat lower towards the valance band section of the pristine system. Now, the bands from the conduction band are crossing the Fermi level and reaching the valance band, resulting in overlapping bands and, as a result, a metallic system. Because of the symmetry of the supercell's single vacancy, the linearly crossing bands are separated and lifted slightly above the Fermi level. The orbitals of vacancy mix with the π^* and π bands surrounding the Fermi level.

Figure 3c shows that the bands around the Fermi level are notably different from those in the pristine system. It can also be seen that when Stone-Wales defect is introduced into a silicene sheet, opening of band gap with band width 40 meV occurs which is in agreement with previous study i.e, 33 meV [9]. In this way small amount of SW defect cause opening in band gap, which can be very important for micro-electronic devices.

Energetics of adsorption systems

We investigated for methane gas adsorption in different positions, and geometries (i.e, tripod towards, tripod away and straddle), relaxed them for all the optimized silicene systems, followed by electronic and magnetic properties calculations on most stable configurations. All the results for adsorption energies, band-gap for different system and magnetization observed there is presented in table III along with the distance at which CH_4 is found from supercell.

We found that CH_4 get adsorbed on silicene systems physically with Van-der Waal's force as presence of small adsorption energies and tiny charge transfer amount. As shown in above table adsorption energy for pristine system is less than that of MV defective system but it is more than that of SW defective system. The result of adsorption energy in our pristine system is equivalent to the previous study [28] where they found it to be 0.18 eV. Due to deficiency of Si atom adsorption energy is found more in MV defective silicene. In case of SW defective silicene buckling increases with rotation of Si-Si bond, which decreases adsorption energy. From this study, we conclude that MV defective silicene is better site for Methane gas sensing and storage. Adsorption energy is positive in all cases it means no external energy is required for Methane to be adsorbed in the silicene system. We incorporate Bader method of charge transfer analysis to investigate the how charge density is changed in the system due to adsorption of CH_4 gas molecules on all silicene systems under investigation. It shows the behavior of CH_4 as electron withdrawing gas and we obtained 0.016e, 0.035e, and 0.025e as the values of an electron charge transfer for pristine silicene, MV defective silicene, and SW defective silicene system.

TABLE III: Distance of C-atom form nearest Si-atom (D), Adsorption energies (E_{ad}), Band gap, Magnetization (M), and Fermi Level (F) for pristine and defective silicene supercell after methane gas adsorption

	D (Å)	(E_{ad}) (eV)	Band-gap	M (μ_B/cell)	F (eV)	Charge transfer
Pristine	3.82	0.186	Dirac-cone	0.00	-2.83	0.016e
MV	3.81	0.208	Metallic	1.35	-3.15	0.035e
SW	3.54	0.108	0.034	0.00	-2.84	0.025e

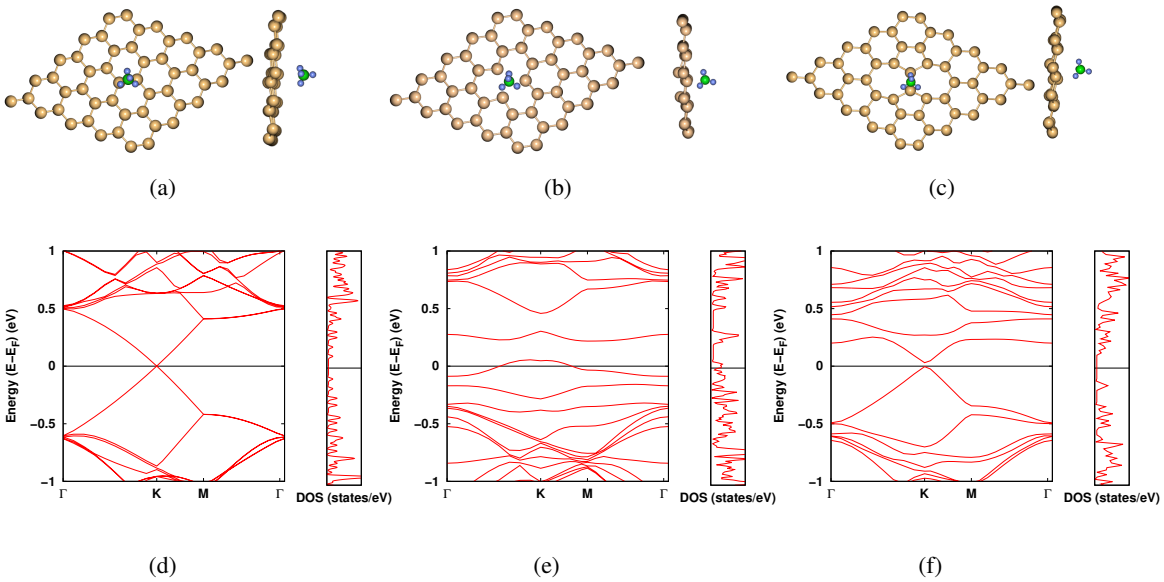

FIGURE 4: Top view and side view of CH_4 adsorbed (a) pristine (b) MV defective (c) SW defective silicene, (where green are C atoms, blue are H atoms and brown are Si atoms); band structure of CH_4 adsorbed (with Fermi level set to zero) (d) Pristine silicene, (e) MV defective silicene and (c) SW defective silicene.

Figures 4 (d, e and f) represents the band structures for pristine and defective system after the adsorption of CH_4 gas. In case of pristine system adsorption of gas does not change the band structure, i.e, there is no change in presence of Dirac-cone after adsorption of methane gas it appears as it is in pristine system. We found similarity in band structures in the case of MV defective silicene system as well. Band structures of MV defective system appears metallic before and after the adsorption of methane gas, which is shown in Figs. 3(b) and 4(e).This shows, the transport of electrons between gas molecules and silicene is negligible. In SW defective system before CH_4 adsorption band gap was found to be 40 meV as shown in Fig. 3(c), which is reduced to 34.1 meV after adsorption of methane gas. In this we found that MV defective silicene can be better system than pristine system but CH_4 adsorption in SW defective system can be useful for tuning band gap.

After band structure calculation, we proceed for density of states as well as projected density of states calculation to study the magnetic properties of the 5×5 supercell of pristine and defective silicene system. Figures 5 (a-c) represent DOS for pristine, MV defective and SW defective 5×5 silicene system after CH_4 gas adsorption. Figures 5 (a) and (c) represent, the distribution of both spin up and spin down states are almost symmetric. Not only that we observed magnetization 0.00 μ_B /cell in our investigation for CH_4 adsorbed pristine and SW defective system. In this way we conclude non-magnetic nature present in pristine and SW defective silicene system remain unchanged even after CH_4 gas adsorption. But, as represented in Fig. 5(b), distribution of density of states for spin up and spin down are not symmetric nearby Fermi level in CH_4 adsorbed MV defective silicene system same as in MV defective silicene. However, from output file we found that magnetization reduced to 1.35 μ_B/cell from 2.00 μ_B/cell due to adsorption of CH_4 gas.This reduction in magnetization shows the decrease in the effects of dangling Si atoms due to presence of C atoms. In this way, we observed that value of total magnetization is reduced due to introduction of CH_4 gas in MV defective system. In other systems i.e, pristine and SW defective silicene systems, no any significant change in DOS is observed after the adsorption of CH_4.

After that we performed the projected density of states (PDOS) computations for various Silicon orbitals. The PDOS plot of a MV defective silicene after CH_4 adsorption is as shown in Fig. 5(d). We can observe from the Projected DOS computations that 3p orbitals are more dominating than 3s orbitals and the non-symmetric form of DOS further confirms the presence of magnetism in the system. Further, we conclude that DOS nearby the Fermi Level have major contribution of 3p orbitals silicon (Si) followed by 3s orbitals of Si. Contribution of 1s orbital of hydrogen and 2s and 2p orbitals of carbon are very less in comparison to that of orbitals of Si.

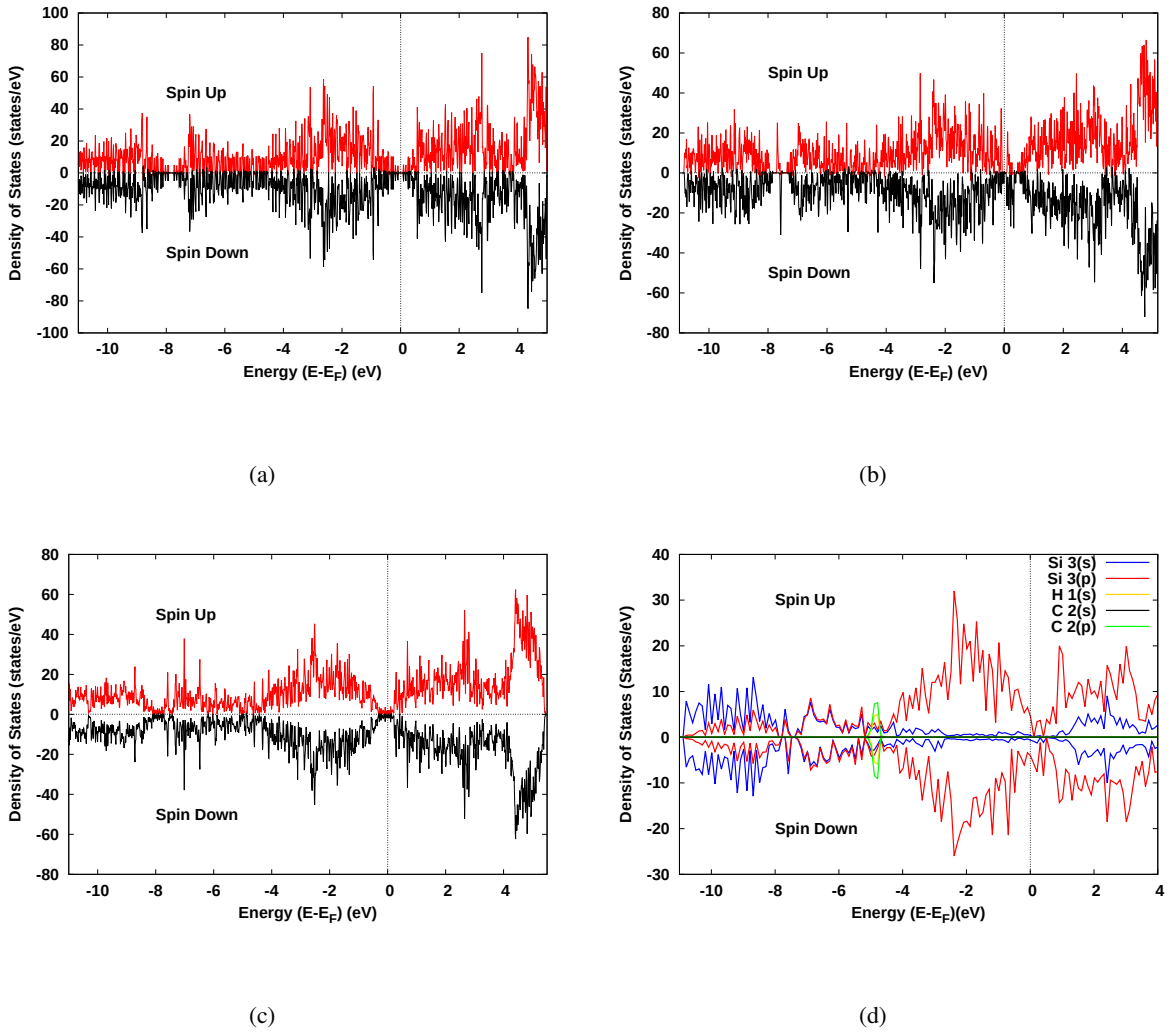

FIGURE 5: DOS for (a) pristine (b) MV defective (c) SW defective silicene system after CH_4 adsorption; (d) PDOS for MV defective silicene after CH_4 adsorption

From all of this we come to the conclusion that introduction of defects play important role in electronic and magnetic properties of silicene system. Further, adsorption of gas molecule does not produce significant changes in pristine and SW defective system in comparison to MV defective system.

CONCLUSIONS

We used first-principles calculations to explore the stability, electronic, and magnetic properties of pure silicene, MV defective silicene, and SW defective silicene, followed by methane gas adsorption in all three systems. On analyzing the band structure of MV defective silicene, we observed the shift of Fermi-level towards the valance band area, thus creating the overlap of bands and hence making the system fully metallic. We observed MV defective silicene is metallic with 2.00 μ_B/cell magnetic moments, while SW defective silicene have band gap of 40 meV and 0.00 μ_B/cell magnetic moments. On studying the most stable configuration adsorption energy is found to be 0.186 eV for pristine silicene, 0.208 eV for MV defective silicene and 0.108 eV for SW defective silicene system. On analyzing band structure and DOS plot of gas adsorbed system we found deduction of magnetization in MV defective system otherwise no any significant changes in band structure and DOS calculation in com-

parison to same system before gas adsorption. This shows that transport of electrons between gas molecule and silicene system is negligible. After this work we conclude that methane physically adsorbed in silicene system with weak Van der Waals force and MV defective silicene is better site for methane adsorption than SW defective silicene and pristine silicene. An adsorption strength of $\sim$ 0.2 - 0.5 eV/molecule [29] is optimal for storage applications, here we have observed that the adsorption energy of MV defective system is within this range, which drive us to conclude that MV defective silicene can be promising for storage applications.

ACKNOWLEDGMENTS

The authors acknowledge the TWAS research grants RG 20- 316 for providing computational help and University Grants Commissions for imparting partial funding.

EDITORS' NOTE

This manuscript was submitted to the Association of Nepali Physicists in America (ANPA) Conference 2022 for publication in the special issue of Journal of Nepal Physical Society.

REFERENCES

1. L. D. Landau, "On the theory of phase transitions. i," Phys. Z. Sowjet. **11**, 26 (1937).
2. M. Ashton, J. Paul, S. B. Sinnott, and R. G. Hennig, "Topology-scaling identification of layered solids and stable exfoliated 2d materials," Phys. Rev. Lett. **118**, 106101 (2017).
3. K. Novoselov, A. Geim, S. Morozov, D. Jiang, Y. Zhang, S. Dubonos, I. Grigorieva, and A. Firsov, "Electric field effect in atomically thin carbon films," Science **306**, 666 (2004).
4. K. Takeda and K. Shiraishi, "Theoretical possibility of stage corrugation in si and ge analogs of graphite," Phys. Rev. B **50**, 14916 (1994).
5. G. Guzman-Verri and L. Lew Yan Voon, "Electronic structure of silicon-based nanostructures," Phys. Rev. B **76**, 075131 (2011).
6. S. Cahangirov, M. Topsakal, E. Aktürk, H. Şahin, and S. Ciraci, "Two- and one-dimensional honeycomb structures of silicon and germanium," Phys. Rev. Lett. **102**, 236804 (2009).
7. M. Houssa, G. Pourtois, V. V. Afanas'ev, and A. Stesmans, "Can silicon behave like graphene? a first-principles study," Appl. Phys. Lett. **97**, 112106 (2010).
8. L. C. Lew Yan Voon, E. Sandberg, R. S. Aga, and A. A. Farajian, "Hydrogen compounds of group-iv nanosheets," Appl. Phys. Lett. **97**, 163114 (2010).
9. J. Gao, J. Zhang, H. Liu, Q. Zhang, and J. Zhao, "Structures, mobilities, electronic and magnetic properties of point defects in silicene," Nanoscale **5**, 9785 (2013).
10. N. Pantha, P. Bissokarma, and N. P. Adhikari, "First-principles study of electronic and magnetic properties of nickel doped hexagonal boron nitride (h-bn)," Eur. Phys. J. B **93**, 164 (2020).
11. N. Pantha, B. Chauhan, P. Sharma, and N. P. Adhikari, "Tuning structural and electronic properties of phosphorene with vacancies," JNPS **6**, 7 (2020).
12. N. Pantha, K. Ulman, and S. Narasimhan, "Adsorption of methane on single metal atoms supported on graphene: Role of electron back-donation in binding and activation," J. Chem. Phys. **153**, 244701 (2020).
13. P. Hohenberg and W. Kohn, "Inhomogeneous electron gas," Phys. Rev. **136**, B864 (1964).
14. W. Kohn and L. J. Sham, "Self-consistent equations including exchange and correlation effects," Phys. Rev. **140**, A1133 (1965).
15. K. Capelle, "A bird's-eye view of density-functional theory," Braz. J. Phys. **36**, 1318 (2006).
16. W. Koch and M. C. Holthausen, *A Chemist's Guide to Density Functional Theory* (John Wiley & Sons, Ltd, Hoboken, New Jersey, 2001).
17. A. Otero-de-la Roza and E. R. Johnson, "Van der waals interactions in solids using the exchange-hole dipole moment model," Chem. Phys. **136**, 174109 (2012).
18. P. Giannozzi, S. Baroni, N. Bonini, M. Calandra, and *et al.*, "Quantum espresso: a modular and open-source software project for quantum simulations of materials," J. Phys. Condens. Matter **21**, 395502 (2009).
19. P. Giannozzi, O. Andreussi, T. Brumme, and *et al.*, "Advanced capabilities for materials modelling with quantum espresso," J. Phys. Condens. Matter **29**, 465901 (2017).
20. P. Giannozzi, O. Baseggio, P. Bonfà, and *et al.*, "Quantum espresso toward the exascale," J. Chem. Phys. **152**, 154105 (2020).
21. J. P. Perdew, K. Burke, and M. Ernzerhof, "Generalized gradient approximation made simple," Phys. Rev. Lett. **77**, 3865 (1996).
22. "`https://www.quantum-espresso.org/`," (Accessed on February, 2022).
23. B. G. Pfrommer, M. Côté, S. G. Louie, and M. L. Cohen, "Relaxation of crystals with the quasi-newton method," J. Comp. Phys. **131**, 233 (1997).
24. H. J. Monkhorst and J. D. Pack, "Special points for brillouin-zone integrations," Phys. Rev. B **13**, 5188 (1976).
25. B. Campforts and G. Govers, "Keeping the edge: A numerical method that avoids knickpoint smearing when solving the stream power law," J. Geophys. Res **120**, 1189 (2015).
26. W. Tang, E. Sanville, and G. Henkelman, "A grid-based bader analysis algorithm without lattice bias," J. Phys. Condens. Matter **21**, 084204 (2009).
27. B. Feng, Z. Ding, S. Meng, Y. Yao, X. He, P. Cheng, L. Chen, and K. Wu, "Evidence of silicene in honeycomb structures of silicon on ag (111)," Nano Lett. **12**, 3507 (2012).
28. S. M. Aghaei, M. M. Monshi, and I. Calizo, "A theoretical study of gas adsorption on silicene nanoribbons and its application in a highly sensitive molecule sensor," RSC Adv. **6**, 94417 (2016).
29. S. K. Bhatia and A. L. Myers, "Optimum conditions for adsorptive storage," Langmuir **22**, 1688–1700 (2006).